

Investigations on V-defects in quaternary AlInGaN epilayers

J. P. Liu,^{a)} Y. T. Wang, and H. Yang

State Key Laboratory on Integrated Optoelectronics, Institute of Semiconductors,
Chinese Academy of Sciences, P. O. Box 912, Beijing, 100083 China

D. S. Jiang

State Key Laboratory for Superlattices and Microstructures, Institute of Semiconductors,
Chinese Academy of Sciences, P. O. Box 912, Beijing, 100083 China

U. Jahn and K. H. Ploog

Paul-Drude-Institut für Festkörperelektronik, Hausvogteiplatz 5-7, 10117 Berlin, Germany

(Received 20 February 2004; accepted 7 May 2004; published online 17 June 2004)

The characteristics of V-defects in quaternary AlInGaN epilayers and their correlation with fluctuations of the In distribution are investigated. The geometric size of the V-defects is found to depend on the In composition of the alloy. The V-defects are nucleated within the AlInGaN layer and associated with threading dislocations. Line scan cathodoluminescence (CL) shows a redshift of the emission peak and an increase of the half width of the CL spectra as the electron beam approaches the apex of the V-defect. The total redshift decreases with decreasing In mole fraction in the alloy samples. Although the strain reduction may partially contribute to the CL redshift, indium segregation is suggested to be responsible for the V-defect formation and has a main influence on the respective optical properties. © 2004 American Institute Of Physics. [DOI: 10.1063/1.1767959]

Currently, there is a great need of solid-state ultraviolet (UV) emitters for many applications, ranging from biomedical devices to the next generation of solid-state lighting. However, it is very difficult to fabricate a high-performance UV light emitting diode (LED) with AlGaIn quantum wells (QWs) as active layer due to the poor crystal quality. The performance of blue LEDs based on InGaN/GaN QWs, however, is not so sensitive to the crystal quality¹ due to the exciton localization effect. By introducing In into AlGaIn, a similar effect as for InGaN QWs is expected for quaternary AlInGaIn. Therefore, AlInGaIn quaternary alloys have attracted intense research interests regarding its growth, properties, and application in UV emitters.²⁻⁵

Although UV LEDs and laser diodes with AlInGaIn-based quantum well structures have already been demonstrated,⁶⁻⁹ less reports are available on AlInGaIn structural properties and optical characteristics. Several authors have reported that In segregation leads to enhanced luminescence in quaternary AlInGaIn.¹⁰⁻¹² However, little attention has been paid to the microstructure and compositional inhomogeneity in the AlInGaIn layers. In this article, we report on the characteristics of V-defects and In segregation near them in AlInGaIn epilayers. The results contain experimental data of atomic-force microscopy (AFM), transmission electron microscopy (TEM), scanning electron microscopy (SEM), and low-temperature cathodoluminescence (CL). Indium segregation in the vicinity of the V-defect is suggested to be responsible for the V-defect formation and has a main influence on the respective optical properties.

The quaternary AlInGaIn epilayers were grown by low pressure metal-organic chemical vapor deposition (MOCVD) on sapphire substrates. A 3 μm GaN template layer was deposited on the sapphire with a 25-nm-thick low temperature GaN buffer layer, followed by a 250-nm-thick AlInGaIn ep-

ilayer. *In situ* optical reflectometry was used to monitor the growth process and to obtain the epilayer thickness. In the investigated three samples, the Al content was 0.08. The samples differ in the In mole fraction, which amounts to 0.03, 0.05, and 0.07. The alloy composition was measured by Rutherford backscattering spectrometry.

A tapping mode AFM was used to obtain the AFM images. Cross-section TEM was used to study the microstructure of the V-defects. Low temperature CL investigations were performed in an SEM equipped with an Oxford mono-CL2 and He-cooling stage system operating at temperatures between 5 and 300 K. A grating monochromator and a cooled charge-coupled device array were used to disperse and detect the CL signal, respectively.

AFM observations for AlInGaIn epilayer samples with different In compositions were performed. Figure 1(a) shows an AFM image of a $3 \times 3 \mu\text{m}^2$ surface area for the sample with an In mole fraction of 0.07. The surface morphology shows atomic steps besides black hexagonal V-defects. The V-defect is confirmed to be an open hexagonal, inverted

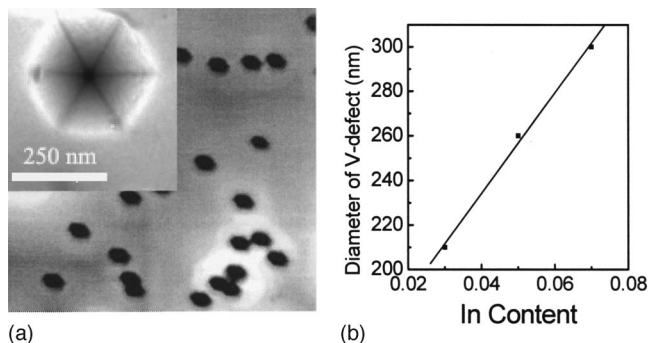


FIG. 1. (a) $3 \times 3 \mu\text{m}^2$ AFM image of the AlInGaIn epilayer sample with an In mole fraction of 0.07. The inset shows a SEM image of a V-defect. (b) Diameter of the V-defect as a function of the In mole fraction in AlInGaIn alloy samples.

^{a)}Electronic mail: jpliu@red.semi.ac.cn

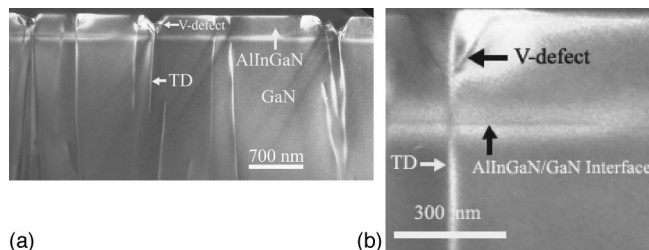


FIG. 2. (a) $(10\bar{1}2)$ cross-section TEM image of the AlInGaN/GaN epilayer with 7% In, which is typically also observed in the other samples. (b) TEM image with a larger magnification containing a V-defect. TD denotes the threading dislocations.

pyramid with $\{10\bar{1}1\}$ side walls as shown by the high-resolution SEM image in the inset. The surface region outside of the V-defects is very smooth, indicating a step-flow growth. The density of V-defects is about $3 \times 10^8 \text{ cm}^{-2}$. Their diameter amounts to about 300 nm on the sample surface. Actually, we have also performed AFM investigations for AlGaIn epilayers grown under comparable conditions (not shown). We could not find any V-defect exists in those samples, although V-defects connected to inversion domains were reported to be possible to form in AlGaIn epilayers in some circumstances.¹³ Consequently, the formation of the V-defects is attributed to the incorporation of In into AlInGaIn. A comparison between AlInGaIn samples with different In mole fraction indicates that the size of the V-defects decreases with decreasing In content as shown in Fig. 1(b), which will be discussed later. Figure 2(a) displays a typical $(10\bar{1}2)$ cross-sectional dark-field TEM image of an AlInGaIn epilayer and of the underlying GaN template layer. It can be seen that each V-defect is associated with a threading dislocation at its apex originating from the underlying GaN template layer as has already been observed in InGaIn/GaN(MQWs).^{14–18} Figure 2(b) shows a TEM image with a larger magnification. It demonstrates that the V-defects are nucleated within the AlInGaIn layer and do not originate from the AlInGaIn/GaN interface, in agreement with our result of AFM section analysis in which the V-defects were also found to be formed within the AlInGaIn layer. The angle between the V-defect facets is about 60° , which agrees well with the angle between two $\{10\bar{1}1\}$ planes.

Figure 3(a) depicts the monochromatic CL image for the AlInGaIn epilayer with an In mole fraction of 0.07. The CL image was measured at 11 K and taken at a wavelength of 384 nm (the peak wavelength of area scan CL is 379.5 nm). The CL image exhibits dark spots surrounded by bright rims. The dark spots correspond to the center of the V-defects. The CL contrast is considered to be mainly related to In composition fluctuation in the alloy and the corresponding shift of the CL peak wavelength. In order to further understand the characteristics of V-defects, a line scan of CL spectra across a V-defect was performed. The electron beam energy was chosen to be 5 keV. Taking the electron scattering and the diffusion length of the excited carriers into account, the diameter of the CL excitation volume and hence the spatial resolution of the CL can be estimated to be about 200 nm. Figure 3(b) shows a series of 20 CL spectra taken across a V-defect as shown by the bright dotted line in Fig. 3(a), which spans a distance of $1.1 \mu\text{m}$. The peak positions and the full widths at half maximum (FWHM) as well as the

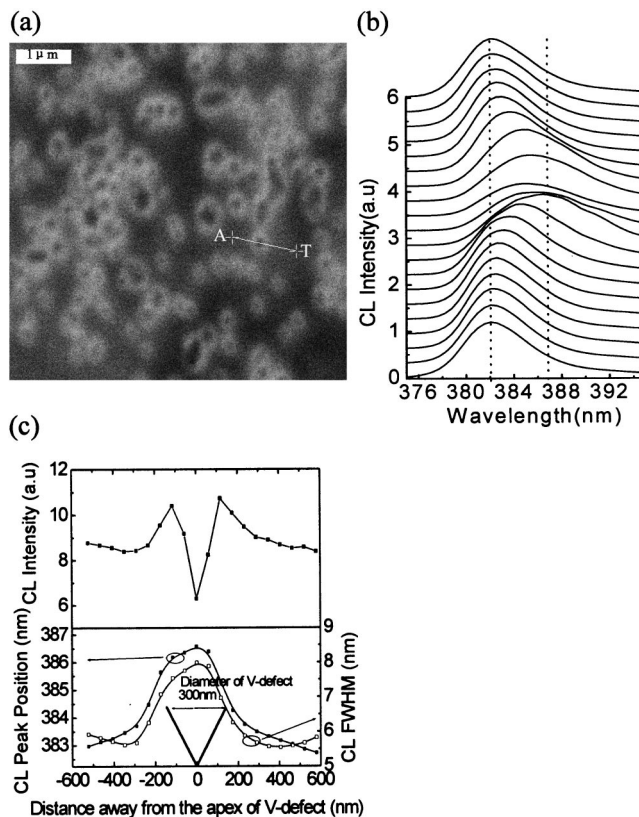


FIG. 3. (a) CL image for the AlInGaIn epilayer with an In mole fraction of 0.07 measured at 11 K and at the wavelength of 384 nm. (b) A series of 20 CL spectra obtained along a line across the V-defect as shown by the bright dotted line in (a). The distance between A and T amounts to $1.1 \mu\text{m}$. (c) The peak wavelength, FWHM, and integrated intensity of the CL spectra along the scanned line. The profile of the V-defect is also schematically shown in the figure.

integral intensity of these CL spectra along with a schematically drawn V-defect profile are shown in Fig. 3(c). For a position of the electron beam about 500 nm away from the center of the V-defect (for example, at the left end of the dotted line marked as A), the peak wavelength is located at 382 nm. The CL peak is redshifted when the measurement spot approaches the apex of the V-defect. At the apex of the V-defect, the CL peak position exhibits the longest wavelength of 386.4 nm, i.e., a total redshift of 4.4 nm compared with the CL peak of spot A, and 6.9 nm compared with the CL peak wavelength obtained by the area scan. Therefore, the CL contrast between the V-defect and its surrounding region is mainly due to the shift of the CL peak wavelength. The main cause of narrowing of the AlInGaIn band gap near the V-defect may be induced by a higher indium concentration near the V-defect. It has been reported that indium atoms tend to segregate in the vicinity of the V-defects in InGaIn alloy.^{16–18} This occurs likewise in AlInGaIn alloy. On the other hand, the formation of V-defects could lead to a partial elastic relaxation of strain.¹⁹ Such a strain relaxation could contribute to the redshift of the CL peak.²⁰ However, it is noted that the In content in our AlInGaIn samples is relatively low, i.e., less than 7%, and the incorporation of Al in the AlInGaIn alloy will partially compensate the lattice mismatch between epilayer and GaN template. The strain reduction induced by V-defects will be much smaller than the case of InGaIn reported by Shi *et al.*²⁰ Therefore, it suggests that the In segregation may be the major cause of redshift of the

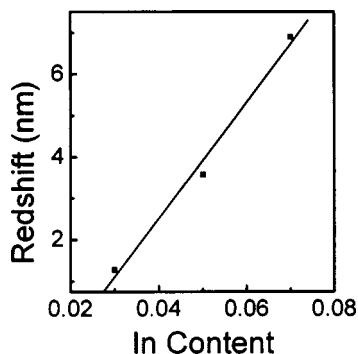


FIG. 4. The total redshift of the CL spectra as a function of the In mole fraction in different AlInGaN samples.

peak wavelength near V-defects in the investigated AlInGaN samples. A careful look at the spectra of Fig. 3(b) shows, however, that the integral CL intensity also changes across the V-defect. It is lower at the center of the V-defect and becomes much higher at the rim, as shown by the curve in the upper part of Fig. 3(c). Moreover, the CL intensity in the rim region is even higher than in the matrix material. The decrease of the CL intensity near the center of the V-defect is at least partly attributed to the enhanced nonradiative recombination due to the threading dislocation at the apex of the V-defect and the off-angle geometry of the V-defect pits. On the other hand, the enhancement of the CL intensity around the V-defect in the rim region may be explained by the gettering effect, i.e., the decreasing concentration of nonradiative impurity centers which migrate toward the threading dislocation resulting in a denuded rim region. It should be noted that during the line scan the FWHM of the CL peak starts to increase at the bright rim region of the V-defect. When the electron beam approaches the apex of the V-defect, the value of FWHM increases, and the largest FWHM is obtained at the apex of V-defect. It is well known that the FWHM of InGaN emission increases with increasing In mole fraction due to the larger fluctuations of the In distribution. Hence, the increase of the FWHM should be related to an increase of the In concentration near the V-defect. In addition, for the samples with different In mole fraction, the observed trend of the changes in the CL peak position and FWHM across V-defects are quite similar to each other, while the amount of the redshift of the CL spectra at the apex of the V-defect depends on the In mole fraction, as shown in Fig. 4. The total redshift value decreases with decreasing In mole fraction of the alloy samples. It confirms that the redshift is mainly related to In segregation even though there is also some influence of the strain reduction.

Combining the structural and optical characteristics of the V-defects, a formation mechanism of V-defects in AlInGaN epilayers is understood as follows. The nucleation of V-defects in AlInGaN is proved to be strongly dependent on the In composition of the samples when the Al composition keeps constant. It is believed that the stress field of the threading dislocation provides a driving force for the migration of indium atoms toward dislocations.¹⁷ The migration induced by stress may lead to the segregation of indium atoms and to the formation of indium-rich clusters near the dislocation. The presence of additional indium significantly reduces the surface energy of the $\{10\bar{1}1\}$ planes,²¹ and thereby leads to the formation of a V-defect exhibiting a

hexahedron cone morphology with sidewalls on $\{10\bar{1}1\}$ planes. The formation of V-defects could lead to a partial strain relief.¹⁹ The V-defects are formed under a critical condition which is dependent on the indium composition in the epitaxial layer and on other growth parameters. When the average In mole fraction of the sample is higher, the In accumulation near the V-defect is more severe resulting in an easier nucleation of V-defects. Thus, V-defects are nucleated at an earlier stage of the growth as compared with lower In mole fractions. This is the reason why V-defects nucleate within the AlInGaN layer, and their geometric size increases with increasing In content.

In summary, we have used AFM, TEM, and low-temperature CL to investigate the characteristics of V-defects in AlInGaN epilayers grown by MOCVD on sapphire. Although the strain reduction may partially contribute to the CL redshift, indium segregation is suggested to be responsible for the V-defect formation and has a main influence on the respective optical properties.

The authors gratefully acknowledge Dr. D. B. Li for his help in TEM measurements and Dr. Y. L. Wang for his help in AFM measurements.

- ¹A. Hangleiter, Phys. Status Solidi C **0**, 1816 (2003).
- ²M. Asif Khan, J. W. Yang, G. Simin, R. Gaska, M. S. Shur, Hans-Conrad zur Loye, G. Tamulaitis, and A. Zukauskas, Appl. Phys. Lett. **76**, 1161 (2000).
- ³J. P. Zhang, J. Yang, G. Simin, M. Shatalov, M. Asif Khan, M. S. Shur, and R. Gaska, Appl. Phys. Lett. **77**, 2668 (2000).
- ⁴A. Chitnis, A. Kumar, M. Shatalov, V. Adivarahan, A. Lunev, J. W. Yang, G. Simin, M. Asif Khan, R. Gaska, and M. Shur, Appl. Phys. Lett. **77**, 3800 (2000).
- ⁵M. Shatalov, A. Chitnis, V. Adivarahan, A. Lunev, J. Zhang, J. W. Yang, Q. Fareed, G. Simin, A. Zakheim, M. Asif Khan, R. Gaska, and M. Shur, Appl. Phys. Lett. **78**, 817 (2000).
- ⁶T. Wang, Y. H. Liu, Y. B. Lee, J. P. Ao, J. Bai, and S. Sakai, Appl. Phys. Lett. **81**, 2508 (2002).
- ⁷A. Yasan, R. McClintock, K. Mayes, S. R. Darvish, P. Kung, and M. Razeghi, Appl. Phys. Lett. **81**, 801 (2002).
- ⁸S. Nagahama, T. Yanamoto, M. Sano, and T. Mukai, Jpn. J. Appl. Phys., Part 1 **41**, 5 (2002).
- ⁹Michael Kneissl, David W. Treat, Mark Teepe, Naoko Miyashita, and Noble M. Johnson, Appl. Phys. Lett. **82**, 2386 (2003).
- ¹⁰H. Hirayama, A. Kinoshita, T. Yamabi, Y. Enomoto, A. Hirata, T. Araki, Y. Nanishi, and Y. Aoyagi, Appl. Phys. Lett. **80**, 207 (2002).
- ¹¹C. H. Chen, L. Y. Huang, Y. F. Chen, H. X. Jiang, and J. Y. Lin, Appl. Phys. Lett. **80**, 1397 (2002).
- ¹²Mee-Yi Ryu, C. Q. Chen, E. Kuokstis, J. W. Yang, G. Simin, and M. Asif Khan, Appl. Phys. Lett. **80**, 3730 (2002).
- ¹³B. Pécz, Zs. Makkai, M. A. di Forte-Poisson, F. Huet, and R. E. Dunin-Borkowski, Appl. Phys. Lett. **78**, 1529 (2001).
- ¹⁴Y. Chen, T. Takeuchi, H. Amano, I. Akasaki, N. Yamada, Y. Kaneko, and S. Y. Wang, Appl. Phys. Lett. **72**, 710 (1998).
- ¹⁵Ig-Hyeon Kim, Hyeong-Soo Park, Yong-Jo Park, and Taeil Kim, Appl. Phys. Lett. **73**, 1634 (1998).
- ¹⁶X. H. Wu, C. R. Elsass, A. Abare, M. Mack, S. Keller, P. M. Petroff, S. P. DenBaars, J. S. Speck, and S. J. Rosner, Appl. Phys. Lett. **72**, 692 (1998).
- ¹⁷Yen-Sheng Lin, Kung-Jeng Ma, C. Hsu, Shih-Wei Feng, Yung-Chen Cheng, Chi-Chih Liao, C. C. Yang, Chang-Cheng Chou, Chia-Ming Lee, and Jen-Inn Chyi, Appl. Phys. Lett. **77**, 2988 (2000).
- ¹⁸N. Duxbury, U. Bangert, P. Dawson, E. J. Thrush, W. Van der Stricht, K. Jacobs, and I. Moerman, Appl. Phys. Lett. **76**, 1600 (2000).
- ¹⁹S. Srinivasan, L. Geng, R. Liu, F. A. Ponce, Y. Narukawa, and S. Tanaka, Appl. Phys. Lett. **83**, 5187 (2003).
- ²⁰L. Shi, C. D. Poweleit, F. A. Ponce, J. Menendez, and W. W. Chow, Appl. Phys. Lett. **79**, 75 (2001).
- ²¹J. E. Northrup, L. T. Romano, and J. Neugebauer, Appl. Phys. Lett. **74**, 2319 (1999).